Cerebral Cortex, July 2017;27: 3869–3878

doi: 10.1093/cercor/bhx094
Advance Access Publication Date: 21 April 2017
Original Article

ORIGINAL ARTICLE

Layer-Dependent Short-Term Synaptic Plasticity Between Excitatory Neurons in the C2 Barrel Column of Mouse Primary Somatosensory Cortex

Sandrine Lefort[1,2] and Carl C.H. Petersen[1]

[1]Laboratory of Sensory Processing, Brain Mind Institute, Faculty of Life Sciences, École Polytechnique Fédérale de Lausanne (EPFL), Lausanne, Switzerland and [2]Department of Basic Neurosciences, University of Geneva, Geneva, Switzerland

Address correspondence to Sandrine Lefort, Department of Basic Neurosciences, University of Geneva, CH-1211 Geneva 4, Switzerland. Email: sandrine.lefort@unige.ch; Carl Petersen, Laboratory of Sensory Processing, Brain Mind Institute, Faculty of Life Sciences, École Polytechnique Fédérale de Lausanne (EPFL), CH-1015 Lausanne, Switzerland. Email: carl.petersen@epfl.ch

Abstract

Neurons process information through spatiotemporal integration of synaptic input. Synaptic transmission between any given pair of neurons is typically a dynamic process with presynaptic action potentials (APs) evoking depressing or facilitating postsynaptic potentials when presynaptic APs occur within hundreds of milliseconds of each other. In order to understand neocortical function, it is therefore important to investigate such short-term synaptic plasticity at synapses between different types of neocortical neurons. Here, we examine short-term synaptic dynamics between excitatory neurons in different layers of the mouse C2 barrel column through in vitro whole-cell recordings. We find layer-dependent short-term plasticity, with depression being dominant at many synaptic connections. Interestingly, however, presynaptic layer 2 neurons predominantly give rise to facilitating excitatory synaptic output at short interspike intervals of 10 and 30 ms. Previous studies have found prominent burst firing of excitatory neurons in supragranular layers of awake mice. The facilitation we observed in the synaptic output of layer 2 may, therefore, be functionally relevant, possibly serving to enhance the postsynaptic impact of burst firing.

Key words: barrel cortex, excitatory postsynaptic potentials, neocortical microcircuits, short-term synaptic plasticity, synaptic transmission

Introduction

The mammalian neocortex contributes to sensory perception, sensorimotor processing, cognition, learning, and memory. In order to understand mechanistically how the neocortex functions, we need to examine the constituent individual neurons and their interactions within the complex neuronal networks of the mammalian brain. Each neocortical neuron receives synaptic inputs from many presynaptic neurons, which are integrated across the somatodendritic arborization. A wiring diagram of synaptic connectivity is of enormous importance for understanding neocortical function, but will not suffice due to nonlinear spatiotemporal integration of the synaptic input and neuromodulatory effects on neuronal network function. The temporal pattern of presynaptic action potentials (APs) dynamically modulates the efficacy of synaptic transmission, a process termed short-term synaptic plasticity. Indeed previous studies have already shown that facilitation and depression are prominent between diverse types of neocortical neurons

(Thomson et al. 1993; Thomson 1997; Tsodyks and Markram 1997; Varela et al. 1997, 1999; Galarreta and Hestrin 1998; Markram et al. 1998; Reyes et al. 1998; Feldmeyer et al. 1999, 2002, 2006; Finnerty et al. 1999; Reyes and Sakmann 1999; Rozov et al. 2001; Petersen 2002; Frick et al. 2007; Jouhanneau et al. 2015; Pala and Petersen 2015). It is likely that different neocortical regions will have different synaptic connectivity, different short-term synaptic plasticity and different dynamic functional activities. Before more general hypotheses can be made, it might therefore be important to examine specific well-defined cortical regions in detail.

Here, we focus on the mouse C2 barrel column, a region of primary somatosensory cortex involved in processing tactile information relating to the C2 whisker (Petersen 2007; Feldmeyer et al. 2013). In vivo measurements of membrane potential (Crochet and Petersen 2006; Poulet and Petersen 2008; Crochet et al. 2011; Gentet et al. 2012; Sachidhanandam et al. 2013; Yamashita et al. 2013), extracellular measurements of AP firing (Guo et al. 2014; Hires et al. 2015; Sofroniew et al. 2015; van der Bourg et al. 2016) and 2-photon calcium imaging (O'Connor et al. 2010; Clancy et al. 2015; Peron et al. 2015; Sofroniew et al. 2015; van der Bourg et al. 2016) are beginning to shed light on the functional operation of the C2 barrel column in awake mice. In order to understand the synaptic mechanisms driving this in vivo activity, we need to examine the dynamic synaptic connectivity of the neurons. An important fraction of the synaptic input to any given neocortical neuron comes from nearby neurons forming a local microcircuit organized in a columnar and laminar fashion. In a previous study, we measured excitatory synaptic connectivity within the mouse C2 barrel column of primary somatosensory cortex finding evidence for layer-specific connectivity (Lefort et al. 2009). In a subset of these recorded neurons, we delivered pairs of presynaptic APs at different interstimulus intervals, and, here, we present the analysis of the short-term synaptic dynamics in these recordings (Lefort et al. 2009) according to the laminar locations of the cell bodies of the presynaptic and postsynaptic neurons.

Materials and Methods

All experiments were carried out in accordance with protocols approved by the Swiss Federal Veterinary Office. In this study, we report the analysis of short-term synaptic plasticity from whole-cell membrane potential recordings of synaptically connected excitatory neurons in the C2 barrel column. These data form a subset of previously reported recordings measuring synaptic connectivity (Lefort et al. 2009), and the methods used to obtain these recordings are described in detail in the previous publication (Lefort et al. 2009). Here, we therefore only briefly describe the methods used for the electrophysiological recordings. Since we did not analyze short-term synaptic plasticity in the previous publication (Lefort et al. 2009), here, we specifically describe in detail only the analysis of short-term synaptic dynamics.

Electrophysiology

C57BL6J mice of both sexes aged P18–21 were anesthetized with 1.5 mg/g urethane and kept at 37 °C on a heating blanket. Intrinsic optical signal imaging was used to identify the location of the C2 barrel column and a drop of fluorescent dye (DiI or SR101) was laid down onto the exposed cortex. Subsequently, 300 µm-thick parasagittal brain slices were cut on a vibratome (Leica VT1000S, Germany) in standard chilled artificial cerebrospinal fluid (ACSF) containing (in mM): 125 NaCl, 2.5 KCl, 25 D-glucose, 25 $NaHCO_3$, 1.25 NaH_2PO_4, 2 $CaCl_2$ and one $MgCl_2$, or in a modified ACSF (Bureau et al. 2006) containing (in mM): 110 choline chloride, 25 $NaHCO_3$, 25 D-glucose, 11.6 sodium ascorbate, 7 $MgCl_2$, 3.1 sodium pyruvate, 2.5 KCl, 1.25 NaH_2PO_4, and 0.5 $CaCl_2$. Slices were then transferred to a chamber filled with standard oxycarbonated ACSF at 35 °C for 15 min followed by a post-incubation period of at least 30 min at room temperature.

Electrophysiological recordings were carried out at 35 °C. Pyramidal or spiny stellate neurons (according to their laminar location and morphology) were visualized with a video microscope (Olympus BX51WI) coupled to a 20×/0.95 NA objective, 4× post-magnification with infrared gradient contrast. Up to 6 simultaneous somatic whole-cell patch-clamp recordings were obtained with Multiclamp 700A amplifiers (Axon Instruments, Molecular Devices). Patch-pipettes (5–7 MΩ) filled with (in mM): 135 K-gluconate, 4 KCl, 4 Mg-ATP, 10 Na_2-phosphocreatine, 0.3 Na-GTP, 10 HEPES (pH 7.3, 280 mOsm) were used. Biocytin (3 mg/ml) was included in the intracellular solution to allow post hoc anatomical reconstruction. Electrophysiological data were Bessel filtered at 5–10 kHz and sampled at 20–40 kHz (ITC-18, Instrutech). Measurements were not corrected for liquid junction potential. The short-term synaptic plasticity stimulation protocol consisted in injecting pairs of brief suprathreshold current pulses into a presynaptic neuron separated by 10 ms, 30 ms, 100 ms, 300 ms, 1 s and 3 s in an interleaved manner with inter-trial intervals of 15 s repeated 20 times for each interstimulus interval. The short-term plasticity measurements were thus recorded over a period of ~30 min, and in some experiments the amplitude of the postsynaptic potentials changed slowly during the recording, typically showing a run-down in both the first and the second postsynaptic potentials. The paired-pulse ratios (PPR) remained stable across the duration of the recordings without significant change in 92% of recordings according to linear correlation analysis across trials.

Analysis and Statistics

Electrophysiological data analysis and statistics were conducted with custom routines written in IgorPro. The resting membrane potential (V_m) and the amplitude of the first unitary excitatory postsynaptic potential (uEPSP) were calculated as described in Lefort et al. (2009). First, the baseline was calculated as an average across 5 ms before the onset of the presynaptic AP. Then, the first uEPSP amplitude was computed as the difference between the mean voltage averaged across 1 ± 0.5 ms around the peak of the first uEPSP and the previously obtained baseline. The second uEPSP waveform for 10, 30, and 100 ms intervals was obtained as follows: all traces from 300 ms to 3 s intervals were averaged and only the first uEPSP of the obtained averaged trace was subtracted from the 10, 30, and 100 ms mean trace. The amplitude of the resulting waveform corresponding to the second uEPSP was calculated as described for the first uEPSP. The PPR for each interval was defined as the ratio between the amplitude of the second uEPSP obtained from the subtracted trace and the first uEPSP. The peak depolarization ratio (PDR) was defined as the ratio between the peak depolarization of the second uEPSP from the original averaged trace (without subtraction) and the first uEPSP. Data are reported in the text and figures as mean ± SEM. In order to determine whether there was statistically significant ($P < 0.05$; see Supplementary Tables) synaptic plasticity, a Wilcoxon signed-rank test for paired data was performed between each distribution and a value of 1. Linear regression analysis was carried out in IgorPro to investigate the relationship between PPR, first uEPSP amplitude and first uEPSP coefficient of variation.

Results

Intralaminar Short-Term Synaptic Plasticity

Simultaneous whole-cell recordings were obtained in vitro from nearby excitatory neurons located within the same neocortical layer of the C2 barrel column, and suprathreshold current pulses were injected into each recorded neuron in turn to test for synaptic connectivity (Lefort et al. 2009). In the example recording shown in Fig. 1A, 3 spiny stellate neurons were recorded in L4, and all 6 possible synaptic connections were found (Lefort et al. 2009). Having identified the synaptic partners, paired-pulse APs interspaced by 10 ms, 30 ms, 100 ms, 300 ms, 1 s, and 3 s were elicited alternately in a presynaptic cell in order to evaluate the short-term dynamics of the synaptic connections (Fig. 1B,C). The amplitude of the second uEPSP for the shortest stimulation intervals (10, 30, and 100 ms) was calculated in 2 steps. First, a reference uEPSP was obtained by averaging all postsynaptic responses corresponding to the 300 ms, 1 s, and 3 s paired-pulse APs. The first uEPSP of this averaged trace was then subtracted from the averaged trace of the 10, 30, and 100 ms, respectively, thus leading to the second uEPSP only (Fig. 1B). In the L4→L4 excitatory synaptic connection example, paired-pulse presynaptic APs at short stimulus intervals evoked a strong depression of synaptic efficacy that progressively recovered as the time between the paired presynaptic APs increases (Fig. 1C). Short-term synaptic plasticity was quantified by calculating the PPR (ratio between the amplitude of the second uEPSP and the first uEPSP; Fig. 1D). We also calculated the PDR as the ratio of the maximal summated depolarization evoked by the second uEPSP and the amplitude of the first uEPSP (Fig. 1D).

In some recordings, we found short-term synaptic facilitation as depicted in an example recording of connected neurons in layer 2 (L2; Fig. 2A). Further, as exemplified for layer 5B (L5B) recordings, different connected neurons within the same layer could show either depression (Fig. 2B) or facilitation (Fig. 2C). There is therefore some diversity of short-term synaptic dynamics within a given cortical layer.

In order to examine this diversity and find out if there are any overall layer-dependent organizing principles, we analyzed short-term synaptic plasticity across many recordings. In general, the strongest short-term plasticity was found at short interstimulus intervals of 10 and 30 ms, with relatively similar effects at both time intervals, and less short-term synaptic plasticity at 100 ms (Fig. 3 and Supplementary Tables 1–3). For intralaminar excitatory synaptic connections with interstimulus interval of 10 ms, we found PPR of (mean ± SEM, median): L2 1.43 ± 0.17, 1.16 (n = 37 pairs), L3 0.83 ± 0.1, 0.74 (n = 21 pairs), L4 0.69 ± 0.03, 0.61 (n = 74 pairs), L5A 0.71 ± 0.08, 0.62 (n = 35 pairs), L5B 1.11 ± 0.13, 1.06 (n = 14 pairs), and L6 0.99 ± 0.28, 1.14 (n = 4 pairs) (Fig. 3 and Supplementary Table 1). Therefore, at the short interstimulus interval of 10 ms, intralaminar excitatory synaptic connections in L2 on average underwent short-term facilitation, whereas depression dominated in L4 and L5A. On average across recordings, there was no significant short-term plasticity at connections within L3, L5B, or L6 (although only a small number of pairs were screened for short-term dynamics in L6).

Overall, similar short-term dynamics were observed at interstimulus intervals of 30 ms, with facilitation dominating for L2 synaptic connections, and depression or no substantial short-term plasticity occurring in other layers (Fig. 3 and Supplementary Table 2). However, spacing consecutive APs by 100 ms decreased the short-term facilitation at intralaminar L2 synaptic connections (Fig. 3 and Supplementary Table 3).

Across recordings, we correlated the PPR with uEPSP1 amplitude and the coefficient of variation of uEPSP1. We found a weak but significant negative correlation of PPR with uEPSP1 amplitude (Supplementary Fig. 1A). We also found a weak but significant positive correlation of PPR with the trial-by-trial coefficient of variation of the amplitude of uEPSP1 (Supplementary Fig. 1B). These data are consistent with the notion that connections with smaller uEPSP1 amplitudes might have lower initial release probability resulting in larger coefficients of variation and stronger facilitation. However, it is important to note that only a small amount of variance across recordings is explained through these correlations.

Summation of first and second uEPSPs at short interstimulus intervals of 10, 30, and 100 ms typically generated peak depolarizations which were larger than the amplitude of the first uEPSP (Fig. 3 and Supplementary Tables 4–6). The PDR at an interstimulus interval of 10 ms was (mean ± SEM, median): L2 2.21 ± 0.16, 1.96 (n = 37 pairs), L3 1.63 ± 0.1, 1.56 (n = 21 pairs), L4 1.51 ± 0.04, 1.49 (n = 74 pairs), L5A 1.54 ± 0.08, 1.53 (n = 35 pairs), L5B 1.92 ± 0.14, 1.91 (n = 14 pairs), and L6 1.86 ± 0.19, 1.88 (n = 4 pairs) (Fig. 3 and Supplementary Table 4). Burst firing of doublets of APs in presynaptic excitatory neurons therefore generated considerably larger depolarization than single APs in postsynaptic excitatory neurons located in the same layer.

Interlaminar Short-Term Synaptic Plasticity

We next examined short-term synaptic plasticity between excitatory neurons located in different layers. The example experiment in Fig. 4A–C shows a synaptic connection between a L4 spiny stellate neuron and a L2 pyramidal neuron, which exhibits short-term synaptic depression at short interstimulus intervals. The example experiment in Fig. 4D–F shows a synaptic connection between a L3 pyramidal neuron and a L5B pyramidal neuron, which exhibits weak synaptic depression. Analyzed across recordings in our interlaminar data set, the most prominent short-term plasticity was found to occur at short interstimulus of 10 and 30 ms, similar to the intralaminar synaptic connections (Fig. 5 and Supplementary Tables 1–3). For interlaminar excitatory synaptic connections with interstimulus interval of 10 ms, we found PPR of mean ± SEM, median: L2→L3 1.34 ± 0.55, 0.92 (n = 3 pairs), L2→L5A 1.29 ± 0.14, 1.23 (n = 12 pairs), L3→L2 1.19 ± 0.25, 0.95 (n = 12 pairs), L3→L5B 0.84 ± 0.12, 0.79 (n = 9 pairs), L4→L2 0.87 ± 0.06, 0.88 (n = 12 pairs), L4→L3 1.05 ± 0.11, 0.94 (n = 10 pairs), L4→L5A 0.99 ± 0.31, 0.53 (n = 13 pairs), L4→L5B 0.54 ± 0.06, 0.55 (n = 6 pairs), L5A→L5B 1.06 ± 0.13, 1.12 (n = 3 pairs), and L5B→L6 1.03 ± 0.19, 0.98 (n = 3 pairs) (Fig. 5 and Supplementary Table 1). For interlaminar synaptic connections at short interstimulus intervals of 10 and 30 ms, presynaptic neurons in L2 tend to give rise to facilitating responses in postsynaptic L5A neurons, whereas presynaptic neurons in L4 synapsing onto L5B neurons tend to give rise to depressing responses. Color-coded PPR matrices help visualize the short-term synaptic plasticity data for both intralaminar and interlaminar excitatory synaptic connections for interstimulus intervals of 10 ms (Fig. 5A), 30 ms (Fig. 5B), and 100 ms (Fig. 5C). Similar to the data for intralaminar synaptic connections, the second uEPSP summated with the first uEPSP at short interstimulus intervals generating PDRs greater than unity at interlaminar synaptic connections (Fig. 5D–F; Supplementary Tables 4–6). In addition to plotting the short-term

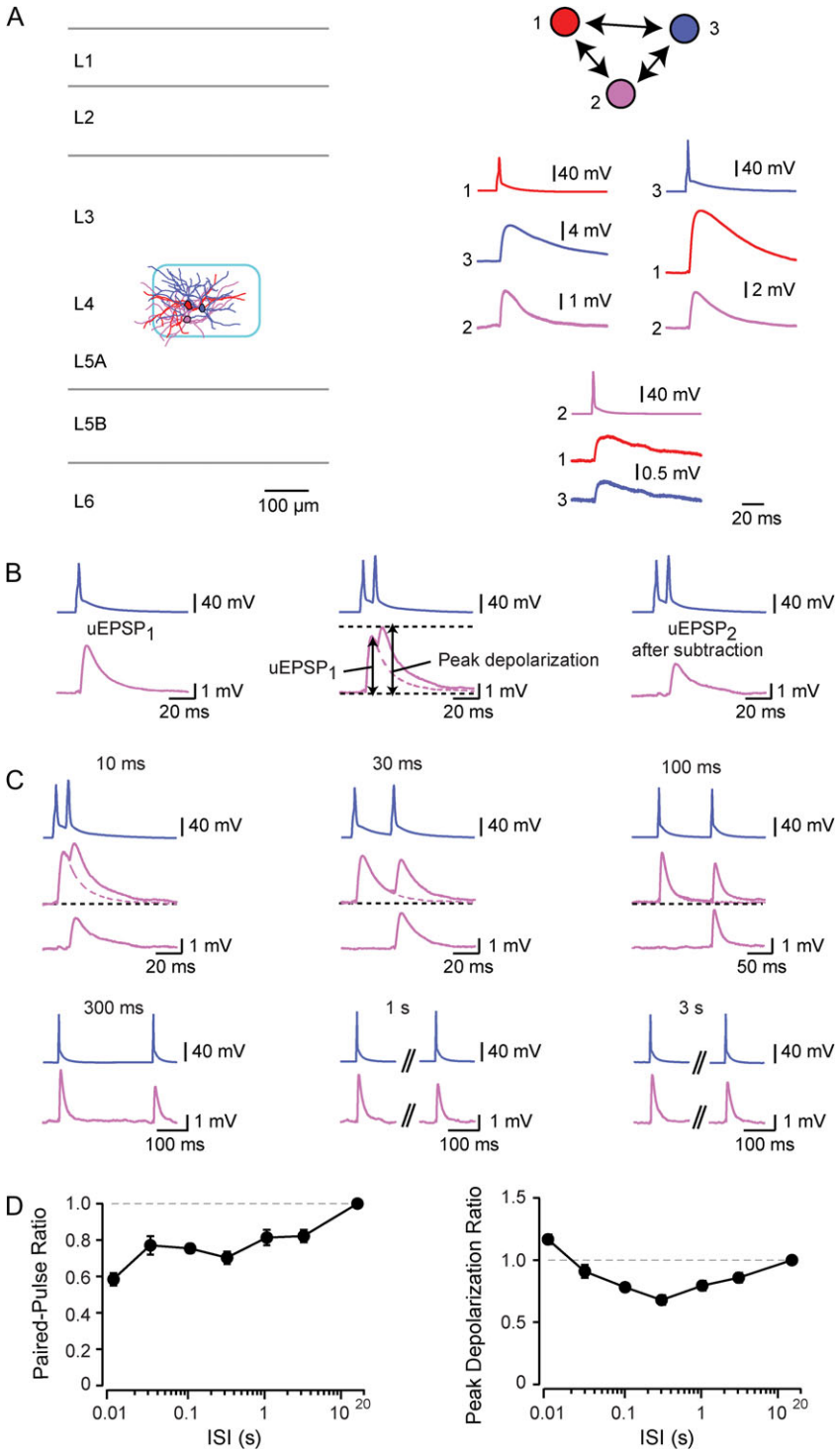

Figure 1. Example of short-term synaptic plasticity between excitatory neurons in layer 4 of the mouse C2 barrel column. (*A*) Example of a recording from L4 spiny stellate neurons within the C2 barrel column. Left: color-coded dendritic reconstructions of the recorded neurons. Right: color-coded schematic connectivity diagram with associated postsynaptic response following a single AP in the presynaptic neurons. (*B*) The short-term plasticity was assessed by evoking paired-pulse APs at different time intervals in the presynaptic neuron. The second postsynaptic potential (uEPSP2) was obtained by subtracting the postsynaptic response to a single AP (uEPSP1). (*C*) Membrane potential responses to paired-pulse stimulation of the L4→L4 synaptic connection at different stimulus frequencies. (*D*) PPR and PDR obtained from this L4→L4 connection (mean ± SEM, $n = 20$ trials).

synaptic plasticity matrices according to layers, we also computed PPR (Fig. 5*G–I*) and PDR (Fig. 5*J–L*) according to the subpial depth of the presynaptic and postsynaptic neurons. This revealed a similar pattern of short-term plasticity with facilitation being most prominent for presynaptic neurons located in the superficial part of the neocortex.

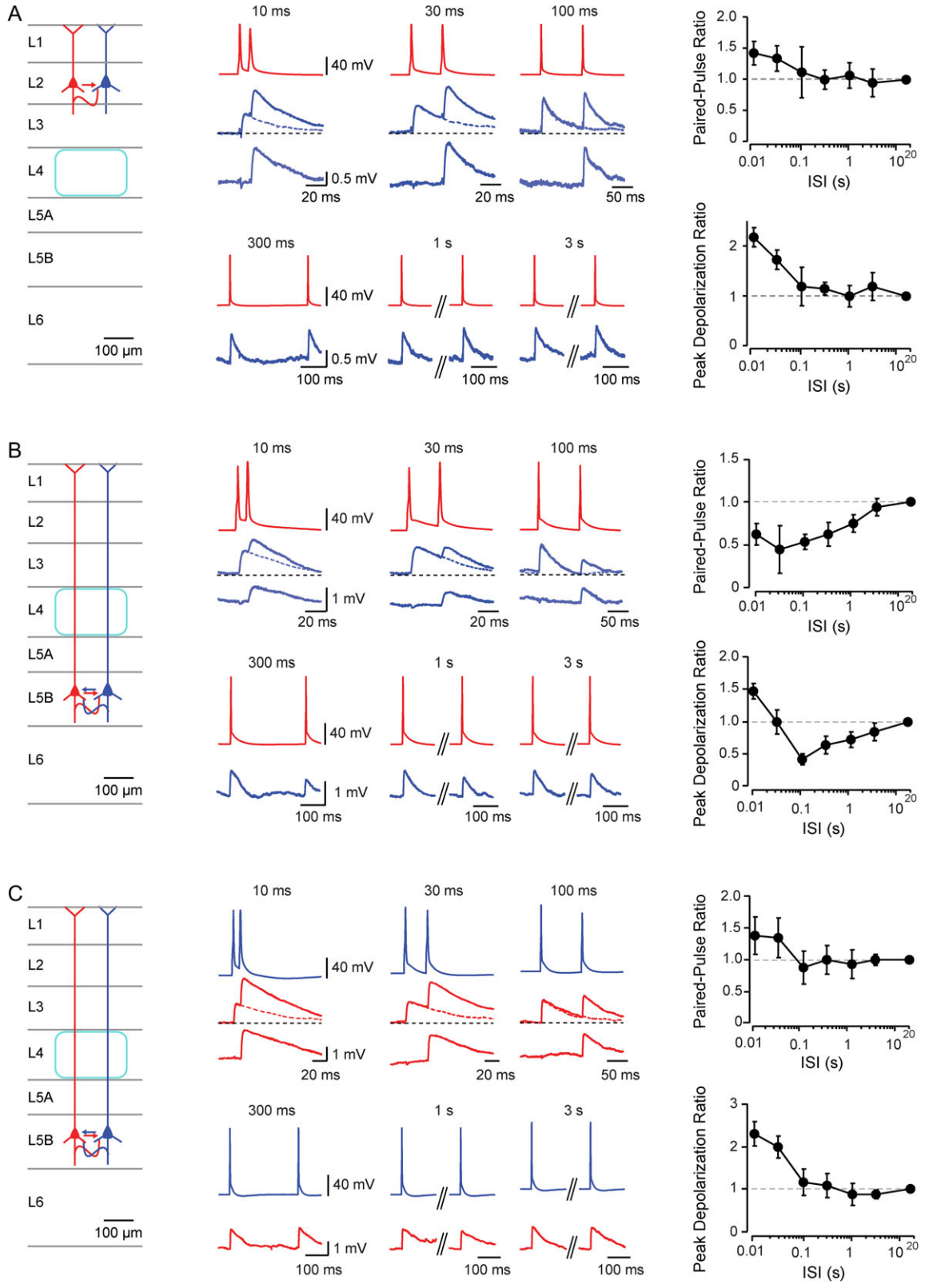

Figure 2. Examples of paired-pulse facilitation and depression at intralaminar synaptic connections in L2 and L5B in the mouse C2 barrel column. (*A*) An example of a L2→L2 synaptic connection showing short-term synaptic facilitation at interstimulus intervals of 10 and 30 ms. (*B*) An example of a L5B→L5B synaptic connection showing short-term synaptic depression. (*C*) The cells shown in panel B were reciprocally connected. The reciprocal connection showed short-term synaptic facilitation at interstimulus intervals of 10 and 30 ms. PPR and PDR are shown as mean ± SEM ($n = 20$ trials).

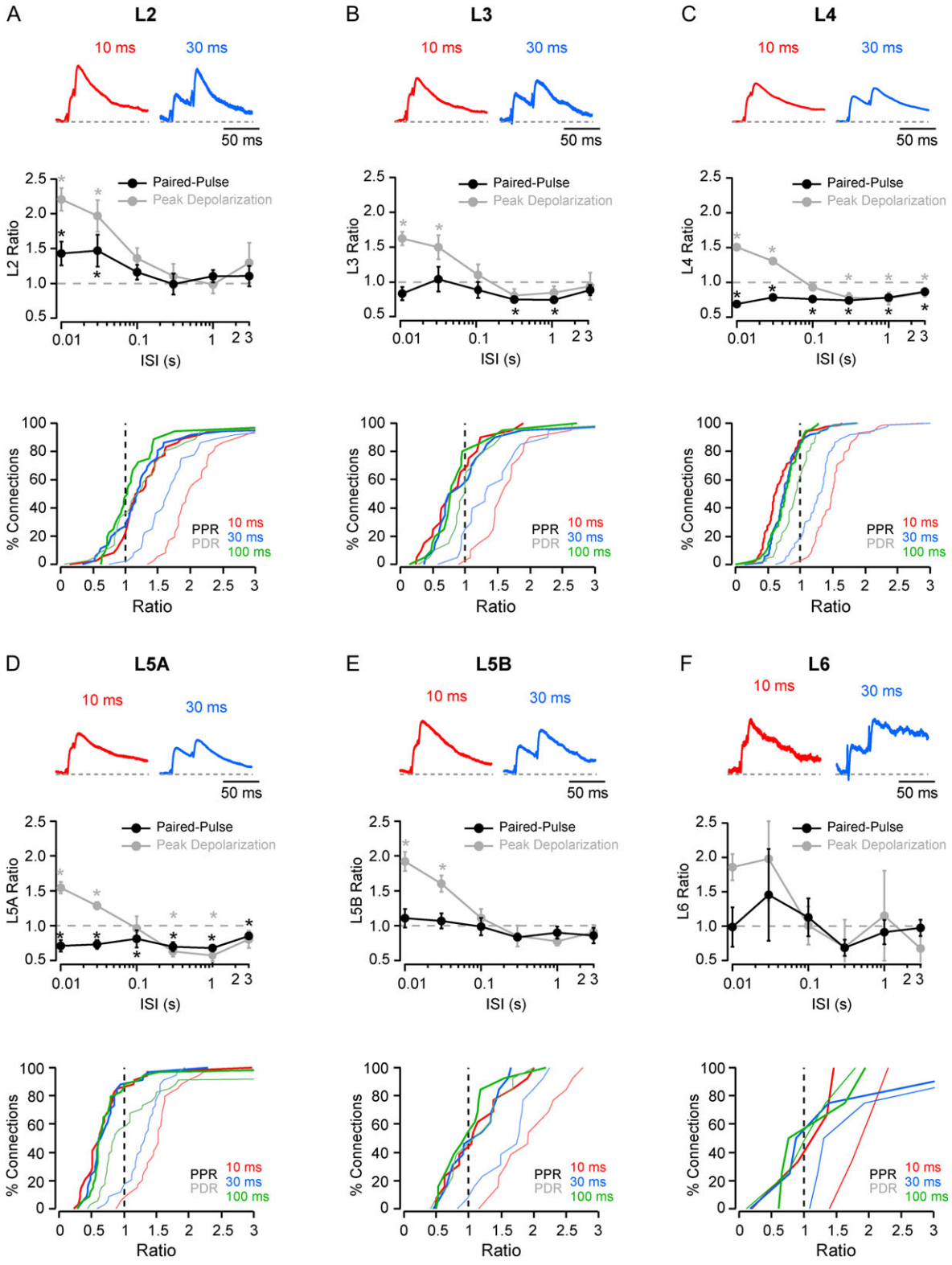

Figure 3. Layer-dependent analysis of intralaminar PPR and PDR for short-term synaptic plasticity at excitatory synapses in the mouse C2 barrel column. (*A*) The post-synaptic responses of L2→L2 synaptic connections ($n = 37$) were normalized to the amplitude of the first EPSP of each synaptic connection and averaged. The grand-average uEPSPs for 10 ms (red) and 30 ms (blue) paired-pulse interstimulus intervals are shown in the upper panel. The time-course of paired-pulse short-term synaptic plasticity across all L2→L2 synaptic connections is shown as the PPR (black) and the PDR (gray) (middle panel), with data presented as mean ± SEM. Statistically significant plasticity is indicated by a * indicating $P < 0.015$. The cumulative distribution of PPR (thick lines) and the PDR (thin lines) for 10 ms, (red), 30 ms (blue), and 100 ms (green) interstimulus intervals (below). (*B*) As for panel A, but for L3→L3 synaptic connections ($n = 21$). (*C*) As for panel A, but for L4→L4 synaptic connections ($n = 74$). (*D*) As for panel A, but for L5A→L5A synaptic connections ($n = 35$). (*E*) As for panel A, but for L5B→L5B synaptic connections ($n = 14$). (*F*) As for panel A, but for L6→L6 synaptic connections ($n = 5$).

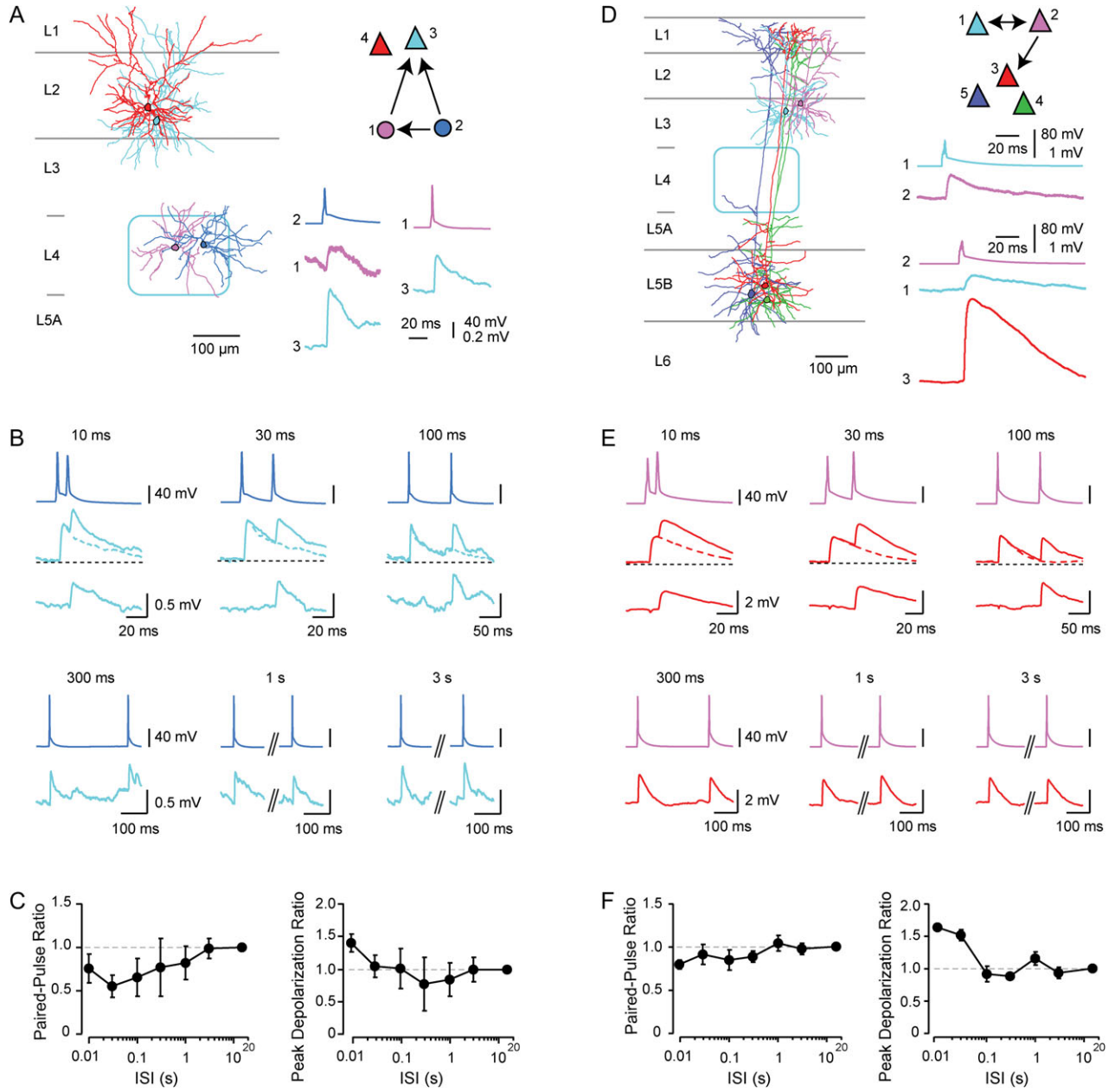

Figure 4. Example experiments investigating interlaminar short-term synaptic plasticity between excitatory neurons in the mouse C2 barrel column. (*A*) In this example experiment, 2 neurons were recorded in L2 and 2 neurons were recorded in L4. Both L4 neurons were presynaptic to one of the L2 neurons. (*B*) The average postsynaptic response of cell 3 located in L2 to different interstimulus intervals of APs applied to cell 2 located in L4. (*C*) PPR and PDR obtained from this L4→L2 example synaptic connection at different interstimulus intervals. Data are shown as mean ± SEM (n = 20 trials). (*D*) A different example showing the connectivity and short-term synaptic plasticity between neurons in L3 and L5B. (*E*) Color-coded postsynaptic responses resulting from different interstimulus intervals of presynaptic paired-pulse stimulation. (*F*) PPR and PDR obtained from this L3→L5B example.

Discussion

Layer-Specific Short-term Synaptic Plasticity

Our data from simultaneous whole-cell recordings of presynaptic and postsynaptic neurons reveal prominent layer-specific short-term synaptic plasticity between excitatory neurons in the C2 barrel column of mouse primary somatosensory cortex. The most prominent synaptic facilitation was observed at L2→L2 and L2→L5A connections. Synaptic depression was prominent at L4→L4, L4→L5B, and L5A→L5A connections. At other synaptic connections, the effects were more varied, either reflecting a real biological variability or a smaller sample size in our study.

Our data are largely in agreement with studies regarding the most commonly investigated synaptic pathways within the barrel cortex. Strong synaptic depression was previously reported at L4→L4 and L5A→L5A synaptic connections in rat barrel cortex, as well as occasional facilitation at short interspike intervals at L2/3→L2/3 synapses (Feldmeyer et al. 1999, 2006; Petersen 2002; Cowan and Stricker 2004; Frick et al. 2008). Some previous reports also found a strong depression at L2/3→L2/3 synapses and a mix of synaptic dynamics at L5A→L5A connections, but

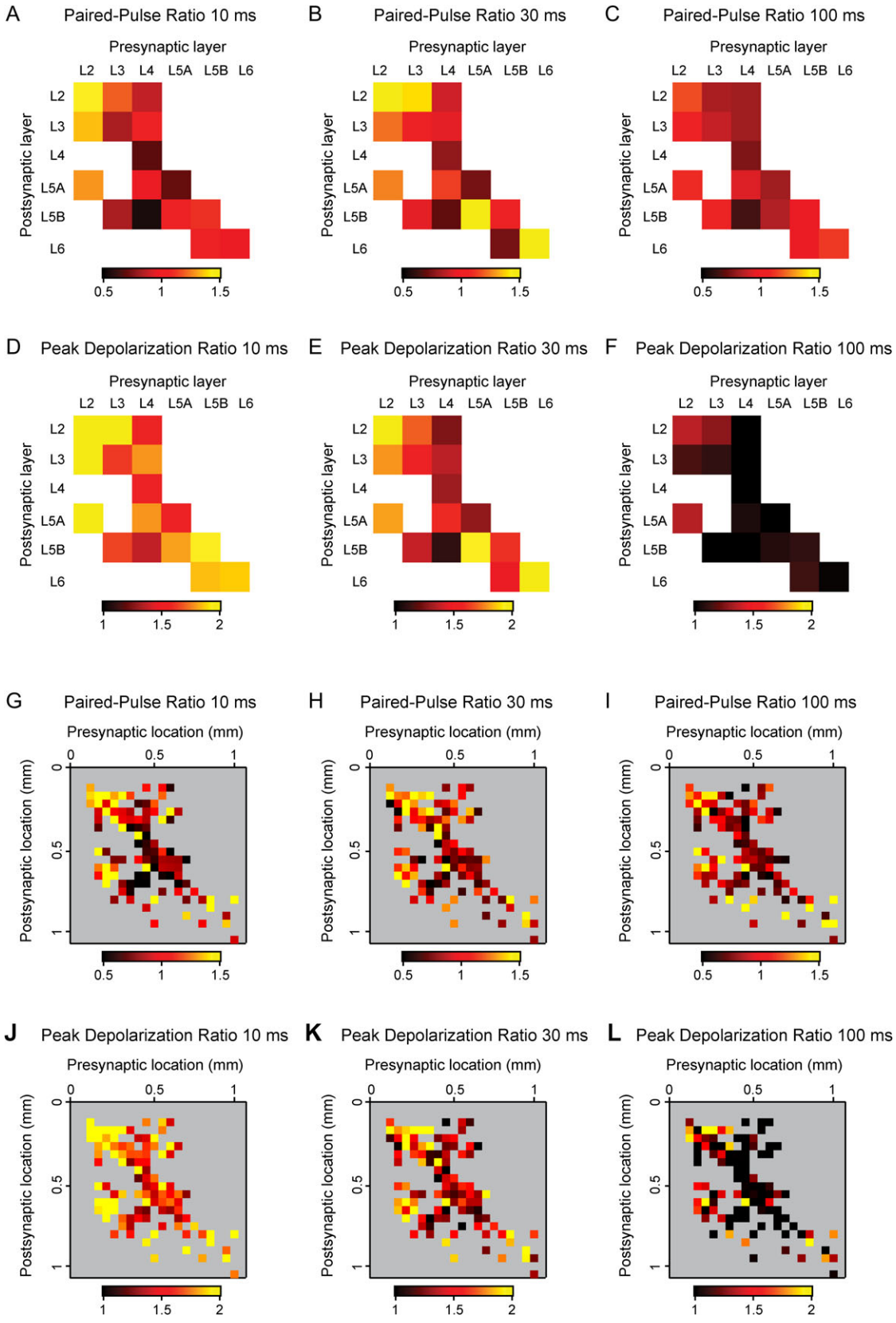

Figure 5. Short-term synaptic plasticity of excitatory synaptic connections in the C2 barrel column. (*A–C*) Color-coded matrices showing the PPR of synaptic connections between neurons in specific layers when the APs were separated by 10, 30, and 100 ms. (*D–F*) Color-coded matrices showing the PDR of synaptic connections between specific layers when the APs were separated by 10, 30, and 100 ms. (*G–I*) same as panels *A–C* except that the matrices are computed based on the presynaptic and postsynaptic location of the recorded neurons with a 50 μm binning in subpial depth. (*J–L*) same as panels *G–I* but for PDR matrices.

these differences may be accounted for by changes in short-term synaptic plasticity during early development (Reyes and Sakmann 1999; Frick et al. 2007; Cheetham and Fox 2010). Short-term dynamic variability among synaptic connections within a given layer can also be due to the different excitatory cell types populating the layer. For instance, a mix of facilitation and depression at L6→L6 synaptic connections has been observed and partly attributed to nonthalamic L6 projecting neurons in the case of depression (Beierlein and Connors 2002).

Possible Functional Relevance

In vivo recordings of identified excitatory pyramidal neurons from barrel cortex of awake behaving mice have typically shown low firing rates, with a few neurons firing at rates well above the median (Petersen and Crochet 2013). Brief bursts or doublets of APs at short interspike intervals have been found to be prominent in L2/3 pyramidal neurons of awake head-restrained mice (Poulet and Petersen 2008) and rats (de Kock and Sakmann 2008). It is of interest to note that in our data set, synaptic facilitation at short interspike intervals of 10 and 30 ms was most prominent at synaptic connections L2→L2 and L2→L5A. The facilitation of postsynaptic potentials induced by burst firing of L2 neurons in awake barrel cortex might therefore contribute to enhancing the importance of synaptic input from L2 to its downstream postsynaptic targets in L2 and L5A. The synaptic facilitation at L2→L2 synapses may also contribute to the relatively long-time scale integration of sensory processing observed in L2 excitatory neurons during active touch (Crochet et al. 2011), especially in L2 neurons projecting to secondary somatosensory cortex (Yamashita et al. 2013).

The short-term synaptic depression, which dominated at L4→L4, L4→L5B, and L5A→L5A connections, may serve to enhance the processing of changes in sensory input, acting as a low-pass filter reducing the postsynaptic impact of repetitive activity within the same presynaptic neurons (Abbott et al. 1997).

Although short-term synaptic plasticity had a strong effect at some synaptic connections, the most robust effects were mediated through temporal summation of uEPSPs. At short interstimulus intervals of 10 and 30 ms, summation of uEPSPs robustly led to PDR greater than unity. Even in the absence of facilitation, burst firing can therefore make an important impact upon postsynaptic targets, and indeed burst firing of L5 pyramidal neurons is thought to be prominent in awake animals (Murayama and Larkum 2009; Xu et al. 2012).

Limitations

There are many limitations to the current study. Most importantly, our measurements were made in vitro from acutely prepared brain slices. It is possible that synaptic plasticity in vivo differs from our in vitro measurements, since the ionic concentrations and presence of various neuromodulators will likely affect synaptic transmission and dynamics. However, a recent in vivo study of synaptic connections between L2 excitatory neurons of mouse barrel cortex found a mean ± SEM PPR of 1.15 ± 0.09 for a mean interspike interval of 14.00 ± 0.84 ms (Jouhanneau et al. 2015), which is in rough agreement with our in vitro measurements of L2 pairs showing PPR of mean ± SEM 1.43 ± 0.17 and median of 1.16 for an interspike interval of 10 ms. The in vivo data were collected under anesthesia (Jouhanneau et al. 2015), which could affect synaptic transmission and plasticity. In the future, it will therefore be important to make measurements in awake mice during different brain states to further examine the physiological properties of synaptic transmission and synaptic dynamics.

Another important drawback of the current study is that we only separated excitatory cell classes according to the laminar position of the cell body, which is likely to mix many different cell types together. For example in L2/3, there are at least 2 different types of excitatory projection neurons, one type projecting to S2 and the other projecting to M1. In infragranular layers, there are many further cell types projecting to different cortical and subcortical targets. It is likely that these cells both have different synaptic connectivity and also different short-term synaptic dynamics (Kiritani et al. 2012). There is, therefore, an enormous amount of further experimental work to be done before we have a complete understanding of excitatory synaptic connectivity and short-term synaptic plasticity in the mouse C2 barrel column.

Supplementary Material

Supplementary data is available at *Cerebral Cortex* online.

Funding

This work was funded by the Swiss National Science Foundation.

Notes

Conflict of Interest: None declared.

References

Abbott LF, Varela JA, Sen K, Nelson SB. 1997. Synaptic depression and cortical gain control. Science. 275:220–224.

Beierlein M, Connors BW. 2002. Short-term dynamics of thalamocortical and intracortical synapses onto layer 6 neurons in neocortex. J Neurophysiol. 88:1924–1932.

Bureau I, von Saint Paul F, Svoboda K. 2006. Interdigitated paralemniscal and lemniscal pathways in the mouse barrel cortex. PLoS Biol. 4:e382.

Cheetham CE, Fox K. 2010. Presynaptic development at L4 to L2/3 excitatory synapses follows different time courses in visual and somatosensory cortex. J Neurosci. 30:12566–12571.

Clancy KB, Schnepel P, Rao AT, Feldman DE. 2015. Structure of a single whisker representation in layer 2 of mouse somatosensory cortex. J Neurosci. 35:3946–3958.

Cowan AI, Stricker C. 2004. Functional connectivity in layer IV local excitatory circuits of rat somatosensory cortex. J Neurophysiol. 92:2137–2150.

Crochet S, Petersen CCH. 2006. Correlating whisker behavior with membrane potential in barrel cortex of awake mice. Nat Neurosci. 9:608–610.

Crochet S, Poulet JF, Kremer Y, Petersen CCH. 2011. Synaptic mechanisms underlying sparse coding of active touch. Neuron. 69:1160–1175.

De Kock CP, Sakmann B. 2008. High frequency action potential bursts (>or= 100 Hz) in L2/3 and L5B thick tufted neurons in anaesthetized and awake rat primary somatosensory cortex. J Physiol. 586:3353–3364.

Feldmeyer D, Brecht M, Helmchen F, Petersen CCH, Poulet JFA, Staiger JF, Luhmann HJ, Schwarz C. 2013. Barrel cortex function. Prog Neurobiol. 103:3–27.

Feldmeyer D, Egger V, Lubke J, Sakmann B. 1999. Reliable synaptic connections between pairs of excitatory layer 4 neurones

within a single "barrel" of developing rat somatosensory cortex. J Physiol. 521:169–190.
Feldmeyer D, Lübke J, Sakmann B. 2006. Efficacy and connectivity of intracolumnar pairs of layer 2/3 pyramidal cells in the barrel cortex of juvenile rats. J Physiol. 575:583–602.
Feldmeyer D, Lübke J, Silver RA, Sakmann B. 2002. Synaptic connections between layer 4 spiny neurone-layer 2/3 pyramidal cell pairs in juvenile rat barrel cortex: physiology and anatomy of interlaminar signalling within a cortical column. J Physiol. 538:803–822.
Finnerty GT, Roberts LS, Connors BW. 1999. Sensory experience modifies the short-term dynamics of neocortical synapses. Nature. 400:367–371.
Frick A, Feldmeyer D, Helmstaedter M, Sakmann B. 2008. Monosynaptic connections between pairs of L5A pyramidal neurons in columns of juvenile rat somatosensory cortex. Cereb Cortex. 18:397–406.
Frick A, Feldmeyer D, Sakmann B. 2007. Postnatal development of synaptic transmission in local networks of L5A pyramidal neurons in rat somatosensory cortex. J Physiol. 585:103–116.
Galarreta M, Hestrin S. 1998. Frequency-dependent synaptic depression and the balance of excitation and inhibition in the neocortex. Nat Neurosci. 1:587–594.
Gentet LJ, Kremer Y, Taniguchi H, Huang ZJ, Staiger JF, Petersen CCH. 2012. Unique functional properties of somatostatin-expressing GABAergic neurons in mouse barrel cortex. Nat Neurosci. 15:607–612.
Guo ZV, Li N, Huber D, Ophir E, Gutnisky D, Ting JT, Feng G, Svoboda K. 2014. Flow of cortical activity underlying a tactile decision in mice. Neuron. 81:179–194.
Hires SA, Gutnisky DA, Yu J, O'Connor DH, Svoboda K. 2015. Low-noise encoding of active touch by layer 4 in the somatosensory cortex. Elife. 4:e06619.
Jouhanneau JS, Kremkow J, Dorrn AL, Poulet JF. 2015. In vivo monosynaptic excitatory transmission between layer 2 cortical pyramidal neurons. Cell Rep. 13:2098–2106.
Kiritani T, Wickersham IR, Seung HS, Shepherd GM. 2012. Hierarchical connectivity and connection-specific dynamics in the corticospinal-corticostriatal microcircuit in mouse motor cortex. J Neurosci. 32:4992–5001.
Lefort S, Tomm C, Sarria JCF, Petersen CCH. 2009. The excitatory neuronal network of the C2 barrel column in mouse primary somatosensory cortex. Neuron. 61:301–316.
Markram H, Wang Y, Tsodyks M. 1998. Differential signaling via the same axon of neocortical pyramidal neurons. Proc Natl Acad Sci USA. 95:5323–5328.
Murayama M, Larkum ME. 2009. Enhanced dendritic activity in awake rats. Proc Natl Acad Sci USA. 106:20482–20486.
O'Connor DH, Peron SP, Huber D, Svoboda K. 2010. Neural activity in barrel cortex underlying vibrissa-based object localization in mice. Neuron. 67:1048–1061.
Pala A, Petersen CCH. 2015. In vivo measurement of cell-type-specific synaptic connectivity and synaptic transmission in layer 2/3 mouse barrel cortex. Neuron. 85:68–75.
Peron SP, Freeman J, Iyer V, Guo C, Svoboda K. 2015. A cellular resolution map of barrel cortex activity during tactile behavior. Neuron. 86:783–799.
Petersen CCH. 2002. Short-term dynamics of synaptic transmission within the excitatory neuronal network of rat layer 4 barrel cortex. J Neurophysiol. 87:2904–2914.
Petersen CCH. 2007. The functional organization of the barrel cortex. Neuron. 56:339–355.
Petersen CCH, Crochet S. 2013. Synaptic computation and sensory processing in neocortical layer 2/3. Neuron. 78:28–48.
Poulet JFA, Petersen CCH. 2008. Internal brain state regulates membrane potential synchrony in barrel cortex of behaving mice. Nature. 454:881–885.
Reyes A, Lujan R, Rozov A, Burnashev N, Somogyi P, Sakmann B. 1998. Target-cell-specific facilitation and depression in neocortical circuits. Nat Neurosci. 1:279–285.
Reyes A, Sakmann B. 1999. Developmental switch in the short-term modification of unitary EPSPs evoked in layer 2/3 and layer 5 pyramidal neurons of rat neocortex. J Neurosci. 19: 3827–3835.
Rozov A, Burnashev N, Sakmann B, Neher E. 2001. Transmitter release modulation by intracellular Ca2+ buffers in facilitating and depressing nerve terminals of pyramidal cells in layer 2/3 of the rat neocortex indicates a target cell-specific difference in presynaptic calcium dynamics. J Physiol. 531:807–826.
Sachidhanandam S, Sreenivasan V, Kyriakatos A, Kremer Y, Petersen CCH. 2013. Membrane potential correlates of sensory perception in mouse barrel cortex. Nat Neurosci. 16:1671–1677.
Sofroniew NJ, Vlasov YA, Hires SA, Freeman J, Svoboda K. 2015. Neural coding in barrel cortex during whisker-guided locomotion. Elife. 4:e12559.
Thomson AM. 1997. Activity-dependent properties of synaptic transmission at two classes of connections made by rat neocortical pyramidal axons in vitro. J Physiol. 502:131–147.
Thomson AM, Deuchars J, West DC. 1993. Large, deep layer pyramid-pyramid single axon EPSPs in slices of rat motor cortex display paired pulse and frequency-dependent depression, mediated presynaptically and self-facilitation, mediated postsynaptically. J Neurophysiol. 70:2354–2369.
Tsodyks MV, Markram H. 1997. The neural code between neocortical pyramidal neurons depends on neurotransmitter release probability. Proc Natl Acad Sci USA. 94:719–723.
Van der Bourg A, Yang JW, Reyes-Puerta V, Laurenczy B, Wieckhorst M, Stüttgen MC, Luhmann HJ, Helmchen F. 2016. Layer-specific refinement of sensory coding in developing mouse barrel cortex. Cereb Cortex. doi:10.1093/cercor/bhw280.
Varela JA, Sen K, Gibson J, Fost J, Abbott LF, Nelson SB. 1997. A quantitative description of short-term plasticity at excitatory synapses in layer 2/3 of rat primary visual cortex. J Neurosci. 17:7926–7940.
Varela JA, Song S, Turrigiano GG, Nelson SB. 1999. Differential depression at excitatory and inhibitory synapses in visual cortex. J Neurosci. 19:4293–4304.
Xu NL, Harnett MT, Williams SR, Huber D, O'Connor DH, Svoboda K, Magee JC. 2012. Nonlinear dendritic integration of sensory and motor input during an active sensing task. Nature. 492:247–251.
Yamashita T, Pala A, Pedrido L, Kremer Y, Welker E, Petersen CCH. 2013. Membrane potential dynamics of neocortical projection neurons driving target-specific signals. Neuron. 80:1477–1490.